Climatic Change
DOI 10.1007/s10584-010-9888-4

Climate change impacts on the hydrology of a snowmelt driven basin in semiarid Chile

Sebastian Vicuña · René D. Garreaud · James McPhee

Received: 31 October 2008 / Accepted: 2 June 2010

Abstract In this paper we present an analysis of the direct impacts of climate change on the hydrology of the upper watersheds (range in elevation from 1,000 to 5,500 m above sea level) of the snowmelt-driven Limarí river basin, located in north-central Chile (30° S, 70° W). A climate-driven hydrology and water resources model was calibrated using meteorological and streamflow observations and later forced by a baseline and two climate change projections (A2, B2) that show an increase in temperature of about 3–4°C and a reduction in precipitation of 10–30% with respect to baseline. The results show that annual mean streamflow decreases more than the projected rainfall decrease because a warmer climate also enhances water losses to evapotranspiration. Also in future climate, the seasonal maximum streamflow tends to occur earlier than in current conditions, because of the increase in temperature during spring/summer and the lower snow accumulation in winter.

S. Vicuña
Centro Interdisciplinario de Cambio Global, Pontificia Universidad Catolica de Chile,
Vicuna Mackenna 4860, Macul, Santiago, Chile
e-mail: svicuna@uc.cl

R. D. Garreaud (✉)
Department of Geophysics and Advanced Mining Technology Center,
Facultad de Ciencias Físicas y Matemáticas, Universidad de Chile,
Blanco Encalada 2002, Santiago, Chile
e-mail: rgarreau@dgf.uchile.cl

J. McPhee
Department of Civil Engineering and Advanced Mining Technology Center,
Facultad de Ciencias Físicas y Matemáticas, Universidad de Chile,
Blanco Encalada 2002, Santiago, Chile
e-mail: jpmcphee@gmail.com

Published online: 21 August 2010

1 Introduction

There is increasing evidence of present (last 30 years) and future (during twenty-first century) impacts that anthropogenic greenhouse gas emissions have on the global climate, which materialize in continental- and regional-scale changes in temperature and precipitation (see reviews in Christensen et al. 2007). These changes can lead to dramatic variations in the hydrologic regime, affecting both surface and ground water supply. Snowmelt-driven basins in semiarid regions are systems highly sensitive to climate change, because the hydrologic cycle depends on both precipitation and temperature, and because water is already a scarce resource subject to an ever increasing pressure for its use (Barnett et al. 2005). In this paper we present an analysis of the impacts of climate change on the hydrology of the upper watersheds of the Limarí river basin, located in north-central Chile (30° S), which has both critical characteristics mentioned above.

The Limarí basin drains the western side of the Andes Cordillera along a stretch between 30° S and 31.5° S (see Fig. 1) within the semiarid region (the so-called Norte-Chico) bounded by the extremely dry Atacama Desert to the north and Mediterranean central Chile farther south. In this region, the Andes rise to more than 5,000 m ASL within 200 km of the coastline. Consistently, mean annual precipitation exhibits strong spatial variations, ranging from about 100 mm at the coast to about 300 mm at the top of the Andes and a marked decline from south to north. Precipitation is mostly produced by the passage of extratropical cold fronts during austral winter months, with more than 80% of the annual total falling between

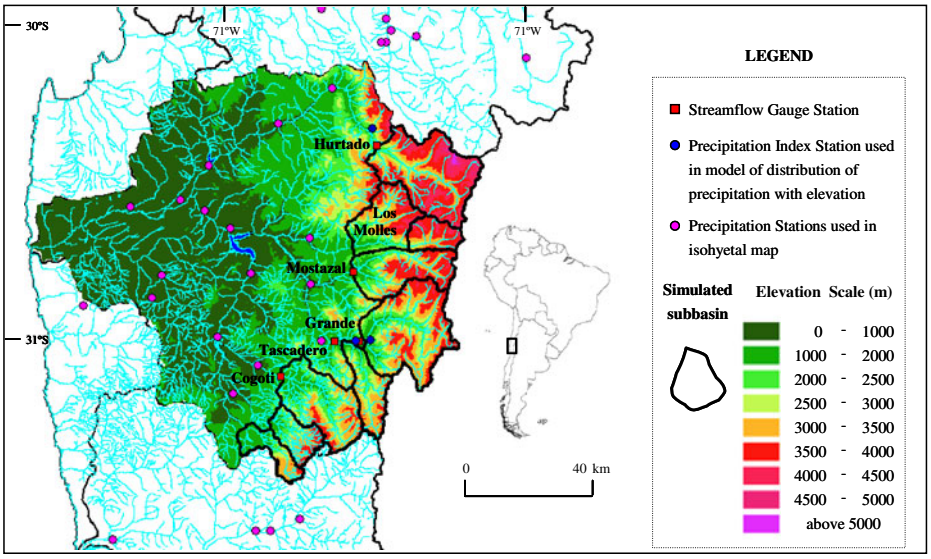

Fig. 1 Topographic map of Limarí basin (elevation scale in *color shaded*). The map also shows precipitation, air temperature and streamflow stations, drainage network, and boundaries of simulated subbasins

May and August (e.g., Falvey and Garreaud 2007). Interannual variability is high (coefficient of variation of 0.7) and strongly linked to ENSO (El Niño Southern Oscillation), whose warm phase is generally associated with higher-than-average precipitation (e.g. Aceituno 1988; Rutllant and Fuenzalida 1991). During the passage of cold fronts, the 0°C isotherm typically is located at about 2,500 m asl (e.g., Garreaud 1992), permitting snow accumulation in the upper half portion of the basins during winter. The upper watersheds in the basins are therefore typically snowmelt-dominated with a large proportion of the streamflow flowing during late spring and summer months (September to January).

Released in early 2007, the fourth Intergovernmental Panel on Climate Change (IPCC) assessment report was based on the results of more than 20 coupled atmosphere-ocean global circulation models (CGCMs) that attempt to characterize the climate by the end of the twenty-first century (2071–2100) under different scenarios of greenhouse gases emissions/concentrations. A cursory inspection of CGCM-based projections of climate change reveals a precipitation decrease and temperature increase for semiarid, north-central Chile (Christensen et al. 2007). It is expected that a reduction of precipitation translates to a reduction of annual mean flow, while an increase in temperature would change the shape of the hydrograph on a basin like Limarí, by moving the flow-weighted timing, or centroid of the hydrograph, earlier in the year (Stewart et al. 2005). This is a consistent result that has been found in other snowmelt dominated regions (Barnett et al. 2005; Vicuna and Dracup 2007).

Although the large number of currently available CGCMs allows examining the consistency of climate projections among the models, most of them have horizontal grid spacing coarser than 200 km, and therefore fail to capture the strong spatial variations in precipitation and temperature that characterize north-central Chile, which are key for representing the hydrological system of these small basins. To improve this representation, we use the outputs from the Providing REgional Climate for Impact Studies (PRECIS; Jones et al. 2004) regional climate model (RCM) that was run with 25-km grid spacing covering all continental Chile. PRECIS was integrated during the 1960–1990 baseline period (BL) and 2071–2100 future period forced by the Hadley Centre Atmospheric Model version 3 (HadAM3; Pope et al. 2001) at its lateral boundaries (Fuenzalida et al. 2007). The future simulations consider IPCC A2 and B2 scenarios of greenhouse gasses concentrations (Nakicenovic and Swart 2000).

The (relatively) high resolution PRECIS outputs are then used to force the Water Evaluation and Planning (WEAP) model (Yates et al. 2005a, b), a climate-driven hydrology and water resources model. WEAP was previously calibrated using historical streamflow observations in the Limarí basin. The impact of future climate change is evaluated by comparing various WEAP outputs between the future scenarios and baseline conditions. Granted, the future conditions will differ from those at present in land-use, vegetation types and water consumption, in addition to changes in climate. We stress that we are only assessing the impact of the climate change (mostly, changes in precipitation and temperature) but this is perhaps the largest signal for the high-elevation, isolated and semiarid basins considered here. The observed and simulated meteorological data is described in Section 2. In Section 3 we describe the WEAP model setup and its calibration. The main results illustrating the hydrological changes between future and present day conditions are presented and discussed in Section 4. Section 5 summarizes our main findings.

Table 1 Meteorological stations used as index stations in distribution model

Station	Watershed(s)	Variable	Elev (m)	LAT	LONG
Pabellon	Hurtado	Precipitation	1,920	30° 24′ 40″ S	70° 33′ 15″ W
Las Ramadas	Grande, Los Molles, Mostazal	Precipitation, temperature	1,380	31° 01′ 05″ S	70° 35′ 08″ W
Tascadero	Tascadero	Precipitation	1,230	31° 00′ 55″ S	70° 39′ 59″ W
Cogoti 18	Cogoti, Pama, Combarbala	Precipitation	840	31° 05′ 01″ S	70° 57′ 00″ W

2 Data

2.1 Observations

Historical hydro-meteorological conditions of the Limarí basin are characterized using data from a network of stations operated by the Dirección General de Aguas (DGA), the government water bureau. Most stations in the dataset have a near-complete monthly-mean record for the period 1970–2000. A set of 21 precipitation stations within the basin and 24 other stations from the neighboring basins are used to create isohyetal maps of annual precipitation. The location of these stations is shown in Fig. 1, and four of them are later used as "index stations" in a model to distribute precipitation spatially. Records of near surface air temperature were available in a network of 6 stations within or near the Limarí basin. Since temperature is more uniformly distributed among subbasins throughout the basin, later on we use only the high-elevation station (Las Ramadas, Table 1) as an index station for monthly temperature. The information in this index station is distributed in the basin considering a vertical temeprature gradient. We also use six streamflow gauges located in the upper watersheds of the Limarí basin, whose location and main characteristics are indicated in Fig. 1 and Table 2, respectively. Because of their placement high in the basin (with minimal diversions farther up) these stations largely measure unimpaired flow (Table 3).

2.2 Regional climate model results

The PRECIS RCM was developed by the Hadley Centre on the basis of the atmospheric component of HadCM3 (Gordon et al. 2000) to generate high resolution climate change scenarios as described in detail by Jones et al. (2004). Three simulations were performed on a domain with 25-km grid spacing that extends from 18° to 57° S and from 85° W to 62° W (Fuenzalida et al. 2007). Simulation baseline (BL)

Table 2 Upper watershed's streamflow gauging stations

Station	Watershed	Surface (km^2)	Elev (m)	LAT	LONG
San Agustin	Hurtado	656	2,035	30° 27′ 00″ S	70° 32′ 00″ W
Ojos de agua	Los Molles	144	2,355	31° 45′ 00″ S	70° 27′ 00″ W
Cuestecita	Mostazal	353	1,250	30° 49′ 00″ S	70° 37′ 00″ W
Las Ramadas	Grande	544	1,380	31° 01′ 00″ S	71° 36′ 00″ W
Dsesembocadura	Tascadero	238	1,370	31° 01′ 00″ S	70° 41′ 00″ W
Fraguita	Cogoti	475	1,065	31° 07′ 00″ S	70° 52′ 00″ W

Table 3 Comparison between meteorological stations and characteristics of PRECIS grids considered to represent the conditions at these stations

Station	Meteorological station			PRECIS grid		
	Elev	LAT	LONG	Average Elev	LAT	LONG
Pabellon	1,920	30° 24′ 40″ S	70° 33′ 15″ W	2,024	30° 30′ 00″ S	70° 45′ 00″ W
Las Ramadas	1,380	31° 01′ 05″ S	70° 35′ 08″ W	2,138	31° 00′ 00″ S	70° 45′ 00″ W
Tascadero	1,230	31° 00′ 55″ S	70° 39′ 59″ W	2,138	31° 00′ 00″ S	70° 45′ 00″ W
Cogoti 18	840	31° 05′ 01″ S	70° 57′ 00″ W	1,055	31° 00′ 00″ S	71° 00′ 00″ W

spans from 1961 to 1990 and intends to represent present-day conditions. Lateral boundary conditions were obtained from the twentieth century integration of the Hadley Centre Atmospheric Model (HadCM3). There is enough overlap between the BL simulation period and the range of historical observations (1970–2000) to consider that their aggregated statistics should represent the same conditions. Further, statistical analysis of the temperature and precipitation series indicate that their means and standard deviation evaluated in both periods (1960–1990/1970–2000) are statistically indistinguishable at the 95% confidence level. It is important to state here that the HadCM3 GCM correctly simulates historic conditions for South America and projections for the future with this model fall within the expected range of results of models used in the latest GCM models intercomparison (Vera et al. 2006).

Simulations A2 and B2 from PRECIS span from 2071–2100 and were laterally forced by results from the A2 and B2 integrations of HadAM3, respectively. A2 and B2 are two widely used IPCC Special Report on Emissions Scenarios (SRES; Nakicenovic and Swart 2000). SRES-A2 is the scenario with the second largest atmospheric CO_2 concentrations by the end of the twenty-first century (about 820 ppmv). In contrast, CO2 concentrations by the end of the century in B2 (about 600 ppmv) fall in the middle of the SRES range.

The PRECIS integration has a time step of a few minutes, generating instantaneous outputs with state variables from which daily and monthly mean and aggregation values are derived. From the two-dimensional fields of precipitation and temperature we chose the grid cells located closest (in a horizontal plane) to the index stations (see Table 3). This procedure can produce significant differences in long-term mean temperature and precipitation over complex terrain. Indeed, PRECIS baseline run (1960–1990) is not a perfect simulation of the present-day climate conditions. Table 4 shows the comparison between long-term annual means (1970–2000 for observations, 1960–1990 for PRECIS BL) of temperature and precipitation for the index stations. PRECIS BL overestimates precipitation by a factor 2–4 and is about 6°C cooler at Las Ramadas station. Nevertheless, the simulated (BL) seasonal cycle of precipitation and temperature are similar to their observed counterparts (Fig. 2), including the extended dry, warm season that characterize semiarid Chile. PRECIS-BL simulation also exhibits interannual variability in precipitation that is in good agreement with the observed variability as measured by the coefficient of variation and the drought persistence metric shown in Table 4.

Based on the previous analysis, it is mandatory to scale PRECIS atmospheric outputs to fit the statistical properties of the observed climate data at the index meteorological stations before using the hydrological model for assessing hydrological changes. For precipitation, we use monthly scale factors (δP_m^{ip}, $m = 1,2,...,12$) for each of the index stations ($ip = 1, 2, 3, 4$), defined as the ratio between the

Table 4 Comparison of statistical properties of observed and simulated climate using GCM (HadBL scenario) historical conditions

Variable	Pabellon		Las Ramadas		Cogoti	
	Observed	HadBL	Observed	HadBL	Observed	HadBL
Annual temperature	N/A		16.4	10.6	N/A	
Annual precipitation	148	662	308	804	182	262
Coefficient of variation (precipitation)	0.69	0.53	0.67	0.52	0.70	0.54
Drought persistence metric[a] (precipitation)	0.22	0.29	0.20	0.27	0.21	0.21

N/A the station is not used as an index station to distribute temperature throughout the subbasins
[a]Defined here as the average of consecutive years of deficit. Deficit is defined as the negative difference between the normalized annual precipitation and 0.75. If a year has a positive difference the deficit is reset to 0

long-term monthly mean of PRECIS BL and the corresponding observed (historical) value. For the temperature index station, the monthly scale (δT_{m}) is defined as the difference between the long-term monthly mean of PRECIS BL and the corresponding observed (historical) value. We then divide (add) the monthly time series extracted from the full PRECIS BL, RA2 and RB2 simulations by the corresponding precipitation (temperature) monthly factors. Hereafter, we only use scaled PRECIS simulations.

3 Model setup

3.1 Hydrologic model development

To study the effects of climate change projections on the hydrology of the Limarí river basin we use the Water Evaluation and Planning (WEAP) model (Yates et al.

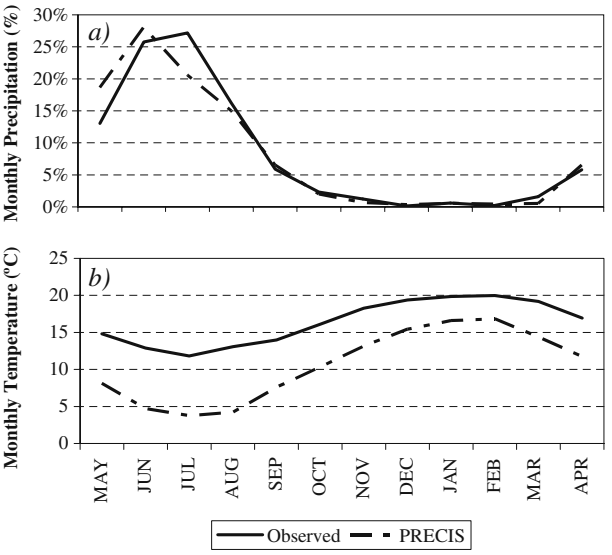

Fig. 2 **a** Observed (*solid*) and PRECIS simulated (*dashed*) long-term monthly fraction of precipitation at Las Ramadas. **b** Observed (*solid*) and PRECIS simulated (*dashed*) long-term monthly mean air temperature at Las Ramadas

2005a, b), a climate-driven hydrology and water resources model. WEAP has been used previously to study the climate change impacts in different basins throughout the world. The most relevant studies to the present work have been the modelling effort done in snowmelt-dominated basins located at the California Sierra Nevada Mountains (Purkey et al. 2008; Jones et al. submitted).

A series of papers (Yates et al. 2005a, b, 2009) describe the manner in which watershed hydrology is integrated into WEAP. In brief, the hydrology module in WEAP is semi-distributed with the study area configured as a contiguous set of sub-catchments that cover the entire extent of a given basin. A climate forcing data set consisting of precipitation, temperature, relative humidity and wind speed is uniformly applied across each sub-catchment, which are fractionally divided into land use/land cover classes. A one dimensional, two-storage soil water accounting scheme uses empirical quasi-physical functions that describe evapotranspiration (potential evapotranspiration is derived using a Penman-Monteith formulation), surface runoff, sub-surface runoff or interflow, and deep percolation (Yates 1996). For a given time step (1 month in this work), values from each fractional area within a sub-catchment are summed to represent the lumped contribution of the sub-catchment to the hydrologic processes for the entire subbasin.

WEAP includes a simple temperature-index snow model which computes effective precipitation and snowmelt considering only two threshold temperatures (melting and freezing) (Yates et al. 2005b). In earlier stages of this work, this simple temperature index algorithm proved to be insufficient to simulate the snow accumulation/melt processes within the upper watersheds of the Limarí basin and hence a modification of this standard algorithm is considered in this work. In the improved algorithm snowmelt is also controlled by the cumulative energy input into the snowpack. The cumulative energy input is a function of the net radiation at the surface level which, in turn, depends on snowpack age and effective albedo. A more detailed description of this algorithm can be found in Young et al. (2009).

GIS layers of land use and topography for the Limarí basin were obtained from a previous modelling work (CAZALAC 2006) and used to develop the basic configuration of the different watersheds considered in the model. With this information we divide each one of the subbasins included in the model (see Fig. 1) into different elevation bands (at 500 m intervals) which allows a better representation of precipitation, temperature and snow accumulation/melt vertical gradients. For each of these elevation bands we classify the catchments into different land uses and assign an initial set of physical parameters to be used in the hydrologic module. Considering the similarities between the two hydrologic regions, the first set of physical parameters is derived from the values used in the models developed in the California Sierra Nevada (Young et al. 2009).

3.2 WEAP calibration

The lack of meteorological stations above 3,000 m ASL in the basin (the maximum height in the basin is over 5,000 m ASL) requires different assumptions on how temperature and precipitation (the main climatic drivers in the model) are distributed with height and location. Three different models are considered for the spatial distribution distributing of precipitation within the basin. The first relies on the annual isohyetal contour map derived using the precipitation amounts

from the stations within and around the basin (see Fig. 1). The second and third methods are constructed by fitting linear and logarithmic functions, respectively, to the relation between precipitation and elevation derived from existing data. After the first trials, we selected the logarithmic model to represent the precipitation-height relationship. This model proved to yield the most realistic estimates of annual runoff. Of course, the logarithmic profile of precipitation is an ad-hoc method for this specific simulation and we do not claim it represents the actual profile for a given storm or season. Nevertheless, results from Favier et al. (2009) and Falvey and Garreaud (2007) based on a more comprehensive (albeit shorter) dataset do support a logarithmic dependence of precipitation with height.

For the distribution of temperature with height we compare the monthly average temperature at two contiguous high elevation stations within a subbasin located in the Elqui river basin (just north of the Limarí basin). We decided to use a monthly temperature gradient after realizing that there are significant differences in this variable for the winter and summer seasons.

Calibration is performed by comparing observed and modeled monthly streamflow at the outlet of six main subbasins (Fig. 1). In terms of the quasi-physical parameters the most relevant are those affecting the snow accumulation and melting processes (which influence streamflow timing) and those related to the ability of the soil to hold and release moisture (important for representing baseflow). Other relevant physical parameters represent soil and vegetation characteristics of the different subbasins. The range of resulting values from the calibration process is shown in Table 5. In this table we present results for the calibration period corresponding to the 1970–1985 period and the validation period corresponding to the 1985–1995 period. The exception would be the Cogoti gauging station where due to lack of data we have considered 1975–1990 and 1990–1995 as the calibration and validation periods. We have included in Table 6 the results for all simulated watersheds and for the validation period for the main watersheds in the basin (which have a long enough record period). The results show that as expected the simulation of streamflow during the validation period has a worse correspondence to observed data. Some reasons behind this worsening in streamflow simulations could be associated with the representation of irrigation conditions. Although irrigation represents a small fraction of the total area it could be altering streamflow in critical months of the year. In our model irrigated land is held static, but considering the time lag

Table 5 Range of parameters resulting from the calibration process

Parameter	Range
Root zone soil water cap (mm)	108–4320
Root zone conductivity (mm/month)	120–900
Deep water capacity (mm)	300–7500
Deep conductivity (mm/month)	140–600
Runoff resistance factor (includes LAI)	0.9–5.85
Melting threshold, t_l (°C)	8
Freezing threshold, t_s (°C)	4
Radiation factor, Rf	0.4–8
Radiation factor (minimum value) (MJ/m^2/d)	7–17
Albedo, new snow, A_N	0.7
Albedo, old snow, A_O	0.3

Table 6 Goodness of fit statistics for six locations with DGA stream flow gauges

In parenthesis we present results for the validation period for the three main subbasins

	Nash-Sutcliff	BIAS (%)
San Agustin	0.74 (0.52)	−2.7 (9.5)
Ojo de Agua	0.66	2.2
Cuestecita	0.69	−0.9
Las Ramadas	0.76 (0.78)	−7.9 (15.8)
Tascadero	0.59	−7.1
Cogoti	0.72 (0.76)	−8.8 (19)

between the calibration and validation periods, there could be some unrepresented differences.

Figure 3 shows the observed and simulated long-term mean monthly streamflow at the six gauging stations. The monthly pattern is correctly simulated by the model, confirming that the snow accumulation and snowmelt process are adequately represented. The monthly mean streamflow time series for the full historical period is presented for three key subbasins in Fig. 4. The model simulations properly represent most of the monthly values with the exception of some low and high flow values where the model tends to over or under estimate the historic conditions,

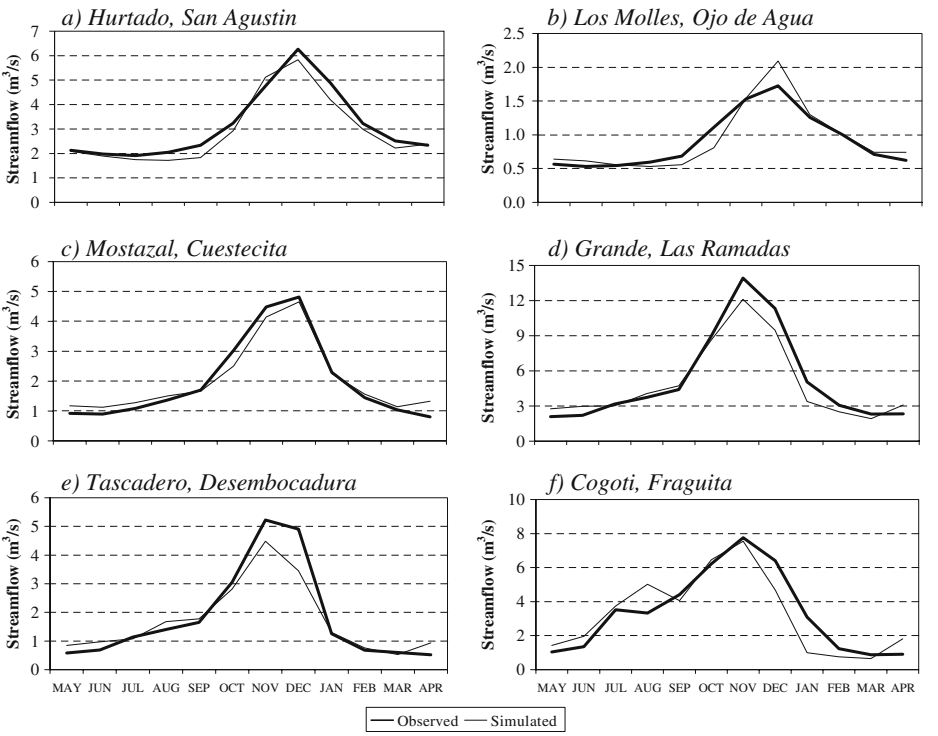

Fig. 3 Observed (*thick line*) and WEAP simulated (*thin line*) long-term monthly mean streamflow at six stations that define the upper subbasins of the Limarí system. Station's name is indicated in each *box*

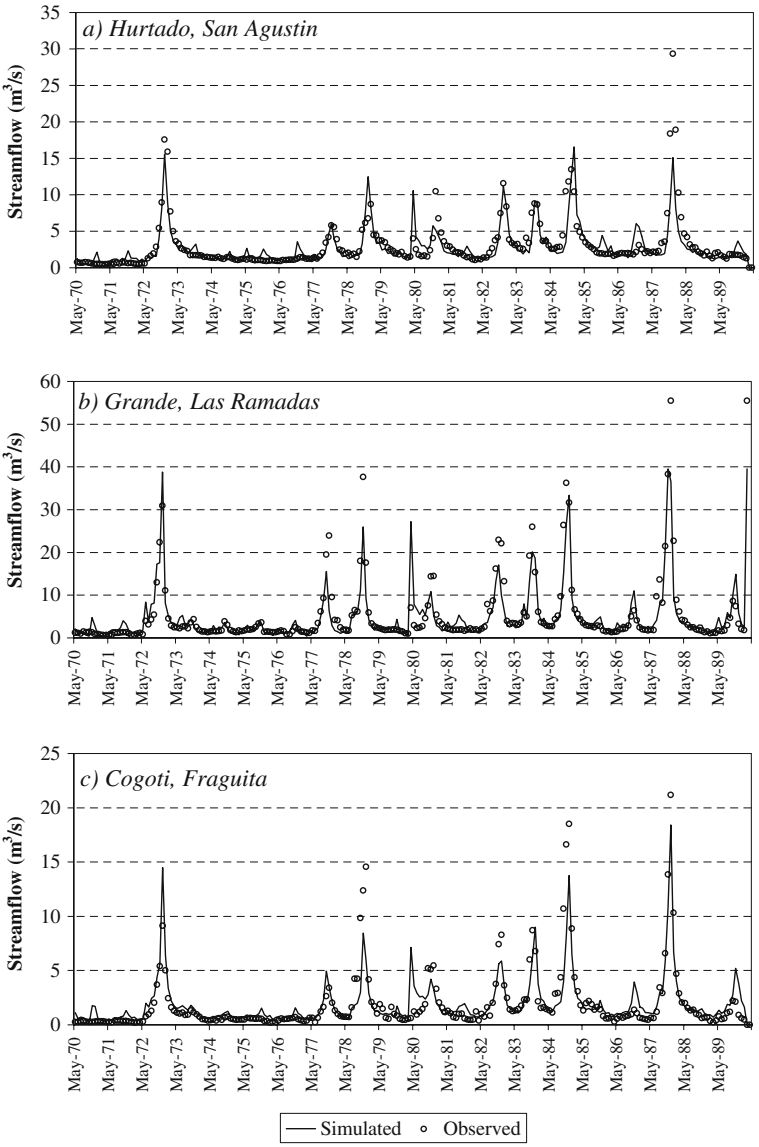

Fig. 4 Observed (*dots*) and WEAP simulated (*line*) monthly streamflow time series at three key Limarí subbasins (name indicated in each *box*)

respectively. In relative terms, low flow underestimation is more significant than high flow overstimation, as can be seen in the scatter plot of the normalized residuales versus observed streamflow in the Grande subbasin (Fig. 5). This over estimation occurs during late spring and summer months in relatively dry years, when the model tends to simulate small but still noticeable snowmelt associated with streamflow accretion that does not occur in reality. The degree of accuracy in the modeling

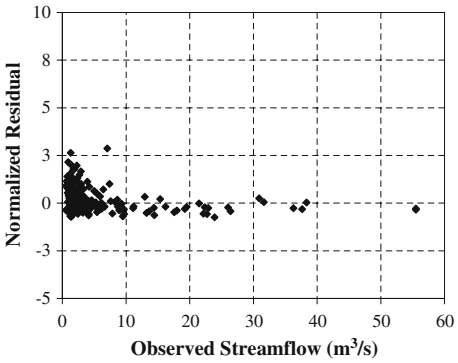

Fig. 5 WEAP simulated minus observed monthly mean streamflow in Río Grande at Las Ramadas as a function of the observed streamflow. The simulation-observation difference was divided by the observed value to produce a normalized residual

results at the monthly timescale is measured using two standard efficiency indices, the Nash Sutcliff and Bias score (Weglarczyk 1998). Results for the six subbasins presented in Table 6 reflect a good level of accuracy with indices of Nash Sutcliff around 0.7–0.8 and bias smaller than 7%.

4 Results

After PRECIS scaling and WEAP calibration, in this section we assess the changes in the hydrologic regime in the Limarí basin under the A2 and B2 climate change scenarios (2070–2090) with respect to the baseline (BL—1960–1990) conditions. Physical, intrinsic parameters associated with land coverage (Table 5) are set equal to the BL conditions, as there is no reason to expect changes in their values because of climate change (e.g., the albedo of fresh snow will remain close to 0.7).

Changes in climate forcing (mainly precipitation and temperature), however, will alter vegetation coveragre and eventually vegetation types. Adressing vegetation-mediated (indirect) climate change upon hydrology would require use of atmosphere-biosphere coupled models of very recent development. In addition, the future will bring changes in water demand and new infrastructure, so one must keep in mind that our WEAP-based study only address the hydrological changes directly related to climate change. We argue, however, that for a largely unpopulated, high-altitude, semiarid basin (75% of the basin covered by bare soil and rocks, the rest being Scleorphyll vegetation), changes in climate forcing represents the largest driver for changes in surface hydrology.

In terms of results from the model we focus in annual and monthly streamflow volumes, potential evapotranspiration, snowpack accumulation and soil moisture. We also compare these results for different subbasins in an attempt to understand how the geographic conditions of a given basin affect the results. Finally, to explore the hydrologic sensitivity of the different subbasins to changes in temperature and precipitation forcing we perform a set of sensitivity experiments in which we hold either temperature or precipitation at their historic levels but considered future values for the remaining forcing variable.

4.1 Full future simulations

Table 7 shows a summary of the three scenarios at annual level for the 2070–2099 timeperiod and Fig. 6 shows the long-term mean hydrograph at each of the six streamflow stations for BL and projected scenarios. Under climate scenarios A2 and B2, the Limarí basin would experience an increase in temperature of about 3–4°C (higher for A2) and a reduction in precipitation of 10–30% (larger for A2) with respect to BL. Precipitation reduction is consistent across subbasins, which leads to a reduction in annual mean streamflow. In relative terms, however, streamflow reductions are larger than those projected for precipitation. Under scenario A2, area-averaged rainfall at the Hurtado subbasin decreases by about a fourth while the estimated decrease in annual streamflow amounts to approximately a third. The amplification in the streamflow response to climate change relative to precipitation forcing is less marked in the Cogoti subbasin (a 19% decrease in precipitation yields a 21% decrease in annual streamflow).

The amplification effect likely results from evapotranspiration enhancement due to temperature increase further reducing the available water for surface flow. Indeed, WEAP predicts an increase in evapotranspiration under scenario A2 of about 30% relative to BL. The enhanced evapotranspiration occurs because potential evapotranspiration increaes with temperature. This amplification factor has been found elsewhere (e.g., Wigley and Jones 1985). We visit this issue in the next section when describing the results from our sensitivity experiments. Also note that the increase in temperature may also lead to enhanced sublimation from the seasonal snowpack, further amplifying the annual mean streamflow reduction. The sublimation is not modeled in WEAP, but the enhanced losses of water from the surface to the air due to any future increase of sublimation is probably an order of magnitude of the enhanced losses due to an increase in evaporation, by virtue of the small fractional

Table 7 Comparison of results for future (2070–2099) and historic (1960–1990) scenarios

Variable	Scenario	Subbasin		
		Hurtado	Grande	Cogoti
Temperature Las Ramadas (°C)	Hist		16.3	
	B2		19.4 (+3.1°C)	
	A2		20.4 (+4.2°C)	
Precipitation (mm/year)	Hist	141	304	199
	B2	127 (−9.9%)	261 (−14.4%)	177 (−10.9%)
	A2	108 (−23.5%)	213 (−29.9%)	161 (−18.8%)
Annual streamflow (m^3/s)	Hist	2.9	4.9	3.1
	B2	2.4 (−19.6%)	3.7 (−23.5%)	2.6 (−16.5%)
	A2	1.9 (−35.5%)	2.9 (−41.5%)	2.4 (−21%)
Summer flow (%)	Hist	48.9	39.4	29.7
	B2	37 (−24.4%)	19.7 (−49.9%)	17.4 (−41.5%)
	A2	33 (−32.5%)	16.6 (−57.8%)	18.2 (−38.6%)
Winter flow (%)	Hist	23.2	25.7	32.5
	B2	29.9 (28.8%)	47.3 (84%)	51.6 (58.9%)
	A2	33.7 (45.3%)	53.5 (108.4%)	56.1 (72.8%)
Centroid (months starting April 15th)	Hist	7.0	6.3	5.7
	B2	6.4 (−8.7%)	5.2 (−17.8%)	4.9 (−13.4%)
	A2	6.2 (−11.7%)	4.9 (−22.5%)	5 (−13.1%)

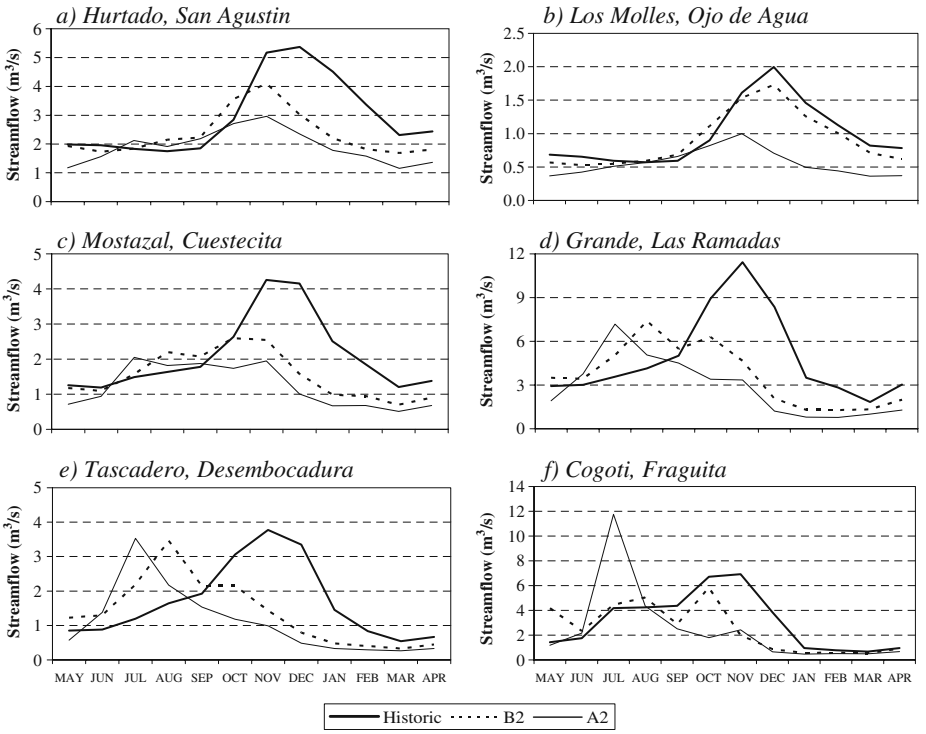

Fig. 6 WEAP simulated long-term monthly mean stream flow at six stations that define the upper subbasins of the Limarí system. WEAP was forced by three climate scenarios (as simulated by PRECIS): baseline conditions (1960–1990; *thick lines*), B2 conditions (2071–2100, *thin dashed lines*) and A2 conditions (2071–2100, *thin solid lines*)

area covered by snow (less than 15%) during the spring summer/season in the basins considered in this study.

Because our study is based in only one atmospheric model (PRECIS forced by HadCM3 under A2 and B2 scenarios) it is not possible to calculate confidence intervals for our hydrological projections. Neverthless, a rough estimate of the uncertanty of our results can be obtained from the uncertainty in annual rainfall changes over this region, the major driver of hydrological changes. For a grid box centered on the Limari basin, considering 22 GCMs used in support of IPCC-AR4 result in a multimodel mean decrease of precipitation (A2/BL) of $31 \pm 7\%$, where the confidence interval is obtained as the standard deviation among the models ($15 \pm 7\%$ when considering B2/BL). Thus, we consider that our projection of a annual mean streamflow reduction (third row Table 7) we suggest considering a $\pm 7\%$ as an uncertainty bound. A complete estimate of WEAP based hydrological uncertainty in future climate is now underway.

Another dramatic change in the hydrological regime of the Limarí basin is the modification of the seasonal cycle of streamflow as can be seen in the mean hydrographs of Fig. 6. There is an increase (decrease) in winter (summer) streamflow as a percentage of annual average with the consequence of an earlier timing of the hydrograph centroid for all basins. These changes are greatly determined by the

subbasin elevation. The highest subbasin, Hurtado at San Agustin (mean elevation of 3,720 m), shows the latest centroid (November 15th) in current climate and its purely snow-dominated regime remains unchanged in the future as the new centroid occurs only 1 month earlier than today. The second highest basin, Grande at Las Ramadas (2,998 m), is also purely snow-dominated under current conditions (late October) but clearly shifts to a mixed regime with peak streamflows during winter months associated with the rainy season (future centroid in August 15th). The lowest subbasin, Cogotí at Fraguita (2,594 m), currently shows a rain-snow dominated regime (centroid at September 1st) and the projected future change in timing is less dramatic as the peak flow already occurs in late winter.

These changes in the hydrograph *between* baseline and A2/B2 are a typical result of increasing temperatures in snowmelt dominated basins (Parry et al. 2007; Vicuna and Dracup 2007) where an increase in temperature leads to a reduction in snowpack accumulation during the rainy season and an earlier, faster snowmelt process during spring and summer. The loss of snowpack in future scenarios is evident in Fig. 7,

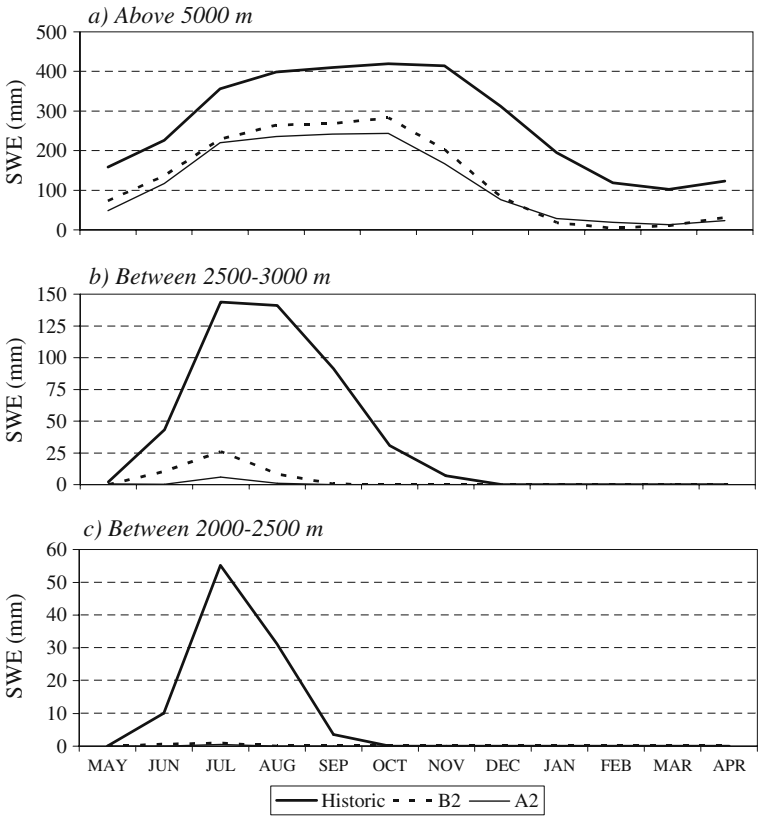

Fig. 7 WEAP simulated long term monthly mean snowpack snow water equivalent (SWE) for three different elevation bands in the Hurtado subbasin. WEAP was forced by three climate scenarios (as simulated by PRECIS): baseline conditions (1960–1990; *thick lines*), B2 conditions (2071–2100, *thin dashed lines*) and A2 conditions (2071–2100, *thin solid lines*)

which shows the snow water equivalent mean annual cycle for three elevation ranges within the Hurtado subbasin. The change in streamflow timing can also be a consequence of reduced snow accumulation during winter. In the current climate, centroid timing in the Limarí basin ranges from late August to early December, and a statistically significant fraction of the interannual variability is accounted for by winter precipitation (Fig. 8) in a linear fashion with a slope of about 1 month per

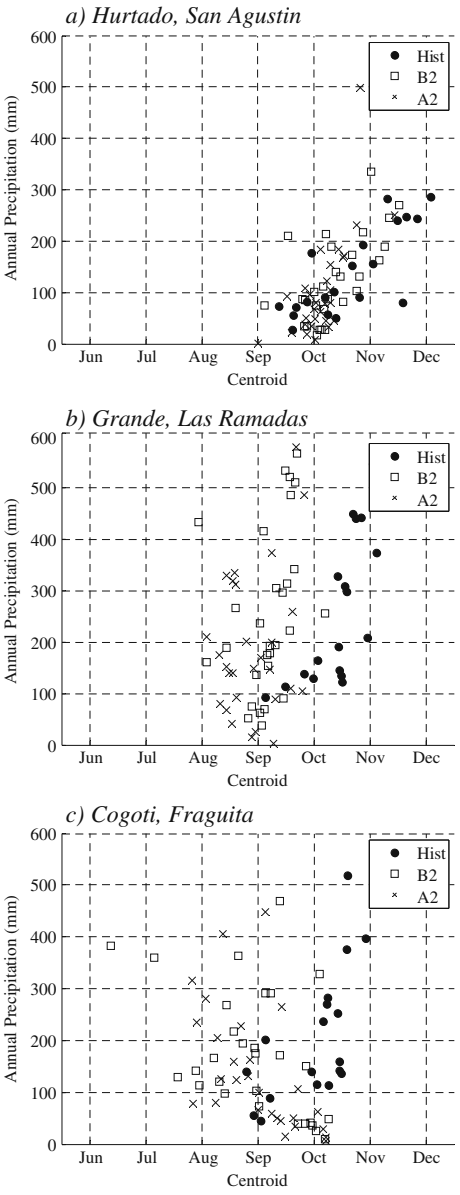

Fig. 8 Scatter plot between WEAP simulated annual precipitation and hydrograph centroid at three key Limarí subbasins (name indicated in each *box*). WEAP was forced by three climate scenarios (as simulated by PRECIS): baseline conditions (1960–1990; *filled circles*), B2 conditions (2071–2100, *empty squares*) and A2 conditions (2071–2100, *crosses*)

100 mm. If winter precipitation is large, the snowpack will feed the rivers during the dry and hot months of late spring and summer. In contrast, a dry winter results in a modest snowpack that quickly melts during the early spring months. The interannual variability of the streamflow timing *within* the 30-year periods in future climate are also controlled by total precipitation (Fig. 8) but such relation weakens in B2 and A2, especially in the lower elevation basins such as the Cogoti. There, the correlation coeffiecient of the linear fit between rainfall and hydrograph centroid is no longer statisicatlly significant and the slope approaches 0 month/mm.

4.2 Sensitivity experiments

In order to further understand the marginal effects of precipitation and temperature changes, we performed two additional experiments. First we consider precipitation at their future conditions (A2) but scaled future temperature to represent historic monthly average values. The second experiment is the opposite: considering temperature at future conditions but scaling future precipitation to represent historic levels. Table 8 presents the results from these experiments. Projected future precipitation combined with historic temperature lead to a reduction of annual streamflow of about 90% of the decrease when considering the full future scenarios (c.f. Tables 7 and 8). This indicates that the amplification response of streamflow with respect to rainfall due to enhanced evaporation is about 10% of the total change. Table 8 also shows that hydrograph centroid earlier timing is largely a product of increased temperature.

Intriguingly, an increase in temperature while keeping precipitation at historical values results in an increase of annual stream volume in Cogoti, the lowest subbasin (Table 8). Such increase in temperature does increase potential evaporation year round (Fig. 9a) but also, as noted before, increases the fraction of wintertime streamflow at the expense of summertime streamflow by raising the snowline during winter storms. For a mid-level basin as Cogoti, this implies more (less) soil moisture during winter (summer) months when evaporation is minimum (maximum), leading to a net reduction in the water lost to the atmosphere when integrated trough the year, as shown in Fig. 9b, c. These Figures also show the very dry conditions during

Table 8 Results from two set of experiments holding temperature (precipitation) at historic levels but changing precipitation (temperature) to future levels

Variable	Scenario	Subbasin		
		Hurtado	Grande	Cogoti
Annual streamflow (m^3/s)	Hist	2.9	4.9	3.1
	Prec B2- Temp Hist	2.6 (−10.8%)	4 (−18.1%)	2.7 (−12.9%)
	Prec A2- Temp Hist	2.1 (−27.5%)	3.1 (−36.4%)	2.5 (−18.1%)
	Prec Hist- Temp B2	2.7 (−7.1%)	4.8 (−2.6%)	3.2 (4.7%)
	Prec Hist- Temp A2	2.7 (−6.8%)	4.9 (0.3%)	3.3 (6.8%)
Centroid (months starting April 15th)	Hist	7.0	6.3	5.7
	Prec B2- Temp Hist	6.8 (−2%)	6.1 (−3.6%)	5.6 (−1.6%)
	Prec A2- Temp Hist	6.8 (−2.8%)	6.1 (−3.8%)	5.8 (2.3%)
	Prec Hist- Temp B2	6.4 (−7.6%)	5.4 (−14.6%)	5 (−12.8%)
	Prec Hist- Temp A2	6.2 (−10.5%)	5.2 (−18.4%)	4.9 (−14.1%)

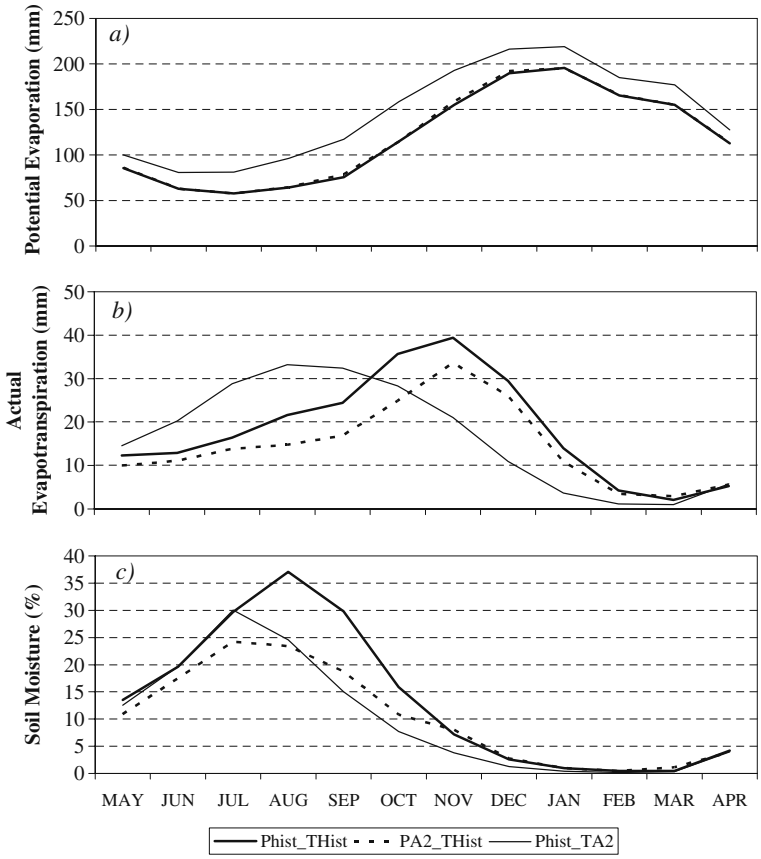

Fig. 9 WEAP simulated long term monthly mean of selected hydrological variables in the Cogoti subbasins: potential evapotranspiration (*upper panel*), actual evapotranspiration (*middle panel*), and soil moisture (*lower panel*). Results of three WEAP simulations are shown: baseline precipitation and temperature (*solid thick lines*), A2-scenario precipitation and scaled baseline temperature (*thin dashed lines*) and scaled baseline precipitation and A2-scenario temperature (*thin solid line*)

spring and summer months that may have potentially dramatic effects in biologic productivity of the ecosystems—an area of potential future research.

To further study this mechanism, we placed "virtual" gauge stations along the Hurtado, Grande and Cogoti rivers, separated every 500 m in the vertical and define a subbasin from there to the Andes ridge. For each of these subbasins we calculated the mean elevation and the annual streamflow change relative to baseline values. The results are shown in Fig. 10. For the Hurtado river, the change is always negative (annual streamflow decrease) because all the subbasins extend high into the Andes, so a warmer condition does not alter substantially the summer to winter fraction of streamflow. In contrast, subbasins that have a mean elevation below 3,000 m, especially those along the Cogoti river, do experience a substantial change in their hydrograph, and exhibit an annual mean flow increase from the mechanism proposed above.

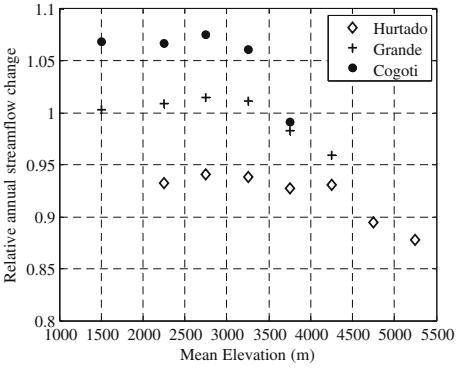

Fig. 10 Relative annual streamflow change (actual change divided by baseline mean value) as a function of subbasin mean elevation along the Cogoti, Hurtado and Grande rivers (see text for further details)

5 Conclusions

Model-based climate projections for the end of twenty-first century indicate substantial warming (increase of 3–4°C) and drying (reductions of 15–35% of present values) along the subtropical Andes. These changes will undoubtedly affect water availability in snowmelt-dominated basins in north-central Chile, with potentially severe consequences in biologic productivity of already precarious ecosystems in these semiarid region. A quantification of the hydrological impacts in the Limarí basin was presented in this study. We used the WEAP hydrology model, previously calibrated with historical data, forced by present-day and future climatic conditions from the PRECIS Regional Climate Model. The PRECIS simulations of future climate were in turn obtained by forcing the model with two IPCC greenhouse gases scenarios (A2 and B2) nested in one GCM, the UKMO HadCM3 model.

As expected, the warmer, drier conditions projected in the A2 and B2 scenarios result in: (a) a reduction of the annual mean streamflow and, (b) a change in the hydrograph with a decreased (increased) streamflow fraction occuring during spring/summer (winter). The fractional reduction in annual streamflow is larger than its precipitation counterpart, because a warmer condition increase evapotranspiration. Hydrograph timing is largely controlled by the increase in temperature, which results in higher snowline during winter storms and earlier, faster snowmelt during spring/summer. The overall precipitation decrease also contributes to a shorter snowmelt season and hence hydrograph change, especially in the two uppermost subbasins.

To understand the marginal effects of increased temperature and precipitation, we conducted two additional experiments, keeping one variable at its historical levels while changing the other to reflect future conditions. Most notably, an increase in temperature does not result in annual streamflow reduction everywhere, in spite that a warmer condition leads to enhanced evapotranspiration. The potential evapotranspiration has a pronounced annual cycle with minimum (maximum) values in winter (summer). Therefore, for relatively low basins, an increase in temperature results in more liquid water input (and hence soil moisture) during winter—when water lost into the atmosphere is at a minimum—and the net effect is an increase in water available for surface runoff.

This work documents, for the first time, the changes that could result from climate perturbations affecting semi-arid Andean watersheds in subtropical South America. There are three important issues that must be addressed in future research. First, in this work we only consider the direct effect of future climate change (specially, temperature increase and precipitation reduction) on surface hiydrology of the Limari basin. Climate change, however, can also alter the vegetation pattern and thus have an indirect effect on hydrology (likely not too large, given the current arid conditions of this area). Secondly, here we only have a crude estimate of the uncertainty of the annual streamflow (based on the uncertainty in precipitation inherited from different GCMs). A more roboust estimate of hydrological uncertainty is needed to explore the full range of seasonal and annual changes in streamflow. Finally, more refined, hourly-resolving hydrological modelling is needed for assesing changes in sub-monthly streamflow, including ocurrence of wintertime floods. This more detailed hydrologic model must capture the nonlinearities inherent to the runoff generation processes, a condition that imposes significant challenges in terms of basic data availability.

Acknowledgements The authors would like to acknowledge the help given in this project by researchers of the Centro de Estudios Avanzados en Zonas Aridas (CEAZA), especially Nicole Kretschmer, Sonia Montecinos and Pablo Alvarez. Also we would like to appreciate the contributions of researchers at the Stockholm Environment Institute in charge of WEAP model developments in especial, Jack Sieber, David Yates, Marisa Escobar and Charles Young. This work was funded by PBCT CONICYT (Chile) grants ACT-19 and Redes-9 and the Advanced Mining Technology Center, Universidad de Chile. Constructive criticisms by two anonymous reviewers greatly improve the content of our work.

References

Aceituno P (1988) On the functioning of the Southern Oscillation in the South American Sector, part I: surface climate. Mon Weather Rev 116:505–524

Barnett TP, Adam JC, Lettenmaier DP (2005) Potential impacts of a warming climate on water availability in snow-dominated regions. Nature 438:303–309

CAZALAC (2006) Aplicación de metodologías para determinar la eficiencia de uso del agua estudio de caso en la región de Coquimbo, Elaborado por CAZALAC; con la asesoría de RODHOS Asesorías y Proyectos Ltda; Gobierno Regional - Región de Coquimbo, p 893

Christensen JH, Hewitson B, Busuioc A, Chen A, Gao X, Held I, Jones R, Kolli RK, Kwon RT, Laprise R, Magaña V, Mearns CG, Menendez CG, Raisanen J, Rinde A, Sarr A, Whetton P (2007) Regional climate projections'. In: Climate change 2007: the physical science basis. Contribution of working group I to the fourth assessment report of the intergovernmental panel on climate change. Cambridge University Press, New York

Falvey M, Garreaud R (2007) Wintertime precipitation episodes in Central Chile: associated meteorological conditions and orographic influences. J Hydrometeorol 8:171–193

Favier V, Falvey M, Rabatel A, Praderio E, López D (2009) Interpreting discrepancies between discharge and precipitation in high-altitude area of Chile's Norte Chico region (26–32°S). Water Resour Res 45:W02424. doi:10.1029/2008WR006802

Fuenzalida H, Aceituno P, Falvey M, Garreaud R, Rojas M, Sanchez R (2007) 'Study on Climate Variability for Chile during the 21st century'. Technical Report prepared for the National Environmental Committee (in Spanish). Available on-line at http://www.dgf.uchile.cl/PRECIS (August 2007)

Garreaud R (1992) Estimación de la altura de la línea de nieve en cuencas de Chile central'. Rev Chil Ing Hidráulica 7:21–32

Gordon C, Cooper C, Senior CA, Banks J, Gregory JM, Johns TC, Mitchell JFB, Wood RA (2000) The simulation of SST, sea ice extent and ocean heat transport in a version of the Hadley Centre coupled model without flux adjustments. Clim Dyn 16:147

Jones RG, Noguer M, Hassell DC, Hudson D, Wilson SS, Jenkins GJ, Mitchell JFB (2004) Generating high resolution climate change scenarios using PRECIS. Met. Office Hadley Center, Exeter, p 40

Nakicenovic N, Swart R (eds) (2000) Special report on emissions scenarios. Cambridge University Press, New York

Parry ML, Canziani OF, Palutikof JP et al (2007) Technical summary. In: Parry ML, Canziani OF, Palutikof JP, van der Linden PJ, Hanson CE (eds) Climate change 2007: impacts, adaptation and vulnerability. Contribution of working group II to the fourth assessment report of the intergovernmental panel' on climate change. Cambridge University Press, Cambridge, pp 23–78

Pope VD, Pamment JA, Jackson DR, Slingo A (2001) The representation of water vapor and its dependence on vertical resolution in the Hadley Centre Climate Model. J Climate 14:3065–3085

Purkey D, Joyce B, Vicuna S, Hanemann M, Dale L, Yates D, Dracup JA (2008) Robust analysis of future climate change impacts on water for agriculture and other sectors: a case study in the Sacramento Valley. Clim Change 87:109–122

Rutllant J, Fuenzalida H (1991) Synoptic aspects of central rainfall variability associated with the Southern Oscillation. Int J Climatol 11:63–76

Stewart IT, Cayan DR, Dettinger MD (2005) Changes toward earlier streamflow timing across Western North America. J Climate 18(8):1136–1155

Vera C, Silvestri G, Liebmann B, González P (2006) Climate change scenarios for seasonal precipitation in South America from IPCC-AR4 models. Geophys Res Lett 33:13

Vicuna S, Dracup JA (2007) The evolution of climate change impact studies on hydrology and water resources in California. Clim Change 82(3–4):327–350

Weglarczyk S (1998) The interdependence and applicability of some statistical quality measures for hydrological models. J Hydrol 206:98–103

Wigley TML, Jones PD (1985) Influences of precipitation changes and direct CO2 effects on streamflow. Nature 314:149–152

Yates D (1996) WatBal: an integrated water balance model for climate impact assessment of river basin runoff. Water Resour Dev 12(2):121–139

Yates D, Sieber J, Purkey D, Huber-Lee A, Galbraith H (2005a) WEAP21: a demand, priority, and preference driven water planning model: part 2, Aiding freshwater ecosystem service evaluation. Water Int 30(4):487–500

Yates D, Sieber J, Purkey D, Huber-Lee A (2005b) WEAP21: a demand, priority, and preference driven water planning model: part 1, model characteristics. Water Int 30(4):501–512

Yates D, Purkey D, Sieber J, Huber-Lee A, Galbraith H, West J, Herrod-Julius S, Young C, Joyce B, Rayej M (2009) Climate driven water resources model of the Sacramento Basin, California. J Water Resour Plan Manage 135(5):303–313

Young CA, Escobar-Arias MI, Fernandes M, Joyce B, Kiparsky M, Mount JF, Mehta VK, Purkey D, Viers JH, Yates D (2009) Modeling the hydrology of climate change in California's Sierra Nevada for subwatershed scale adaptation. J Am Water Resour Assoc (JAWRA) 45(6):1409–1423